Time Scales of Slow Motions in Ubiquitin Explored by Heteronuclear Double Resonance

Nicola Salvi,[†] Simone Ulzega,[†,⊥] Fabien Ferrage,*[,‡,§,‖] and Geoffrey Bodenhausen[†,‡,§,‖]

[†]Ecole Polytechnique Fédérale de Lausanne, Institut des Sciences et Ingénierie Chimiques, BCH, 1015 Lausanne, Switzerland
[‡]Département de Chimie, Ecole Normale Supérieure, 24 rue Lhomond, 75231 Paris Cedex 05, France
[§]Université Pierre et Marie Curie, Paris, France
[‖]UMR 7203 Laboratoire des Biomolécules CNRS-UPMC-ENS, Paris, France

Ⓢ *Supporting Information*

ABSTRACT: Understanding how proteins function at the atomic level relies in part on a detailed characterization of their dynamics. Ubiquitin, a small single-domain protein, displays rich dynamic properties over a wide range of time scales. In particular, several regions of ubiquitin show the signature of chemical exchange, including the hydrophobic patch and the $\beta 4$-$\alpha 2$ loop, which are both involved in many interactions. Here, we use multiple-quantum relaxation techniques to identify the extent of chemical exchange in ubiquitin. We employ our recently developed heteronuclear double resonance method to determine the time scales of motions that give rise to chemical exchange. Dispersion profiles are obtained for the backbone NH^N pairs of several residues in the hydrophobic patch and the $\beta 4$-$\alpha 2$ loop, as well as the C-terminus of helix $\alpha 1$. We show that a single time scale (ca. 50 μs) can be used to fit the data for most residues. Potential mechanisms for the propagation of motions and the possible extent of correlation of these motions are discussed.

The dynamics of proteins are essential to their function:[1] recent evidence, ranging from enzyme catalysis[2−5] to various intermolecular interactions,[6] supports the view that the exploration of the conformational space plays a key role in the mechanism of action of many proteins. NMR is a powerful tool for the study of functional protein dynamics and is established as a method of choice to study motions in biomolecules at atomic resolution.[7,8] Internal motions in ubiquitin have been studied extensively by NMR. Indeed, ubiquitin has been used for two decades as a standard for biomolecular NMR, and new methods have been frequently validated with experiments on ubiquitin. Motions faster than overall tumbling have been characterized in detail[9,10] and can now be reproduced with good accuracy by MD simulations.[11,12] Motions on micro-second−millisecond time scales have been identified,[13−16] and their time scales have been determined for a few residues using several techniques over a range of pH and temperatures.[13,17−20] Motions on time scales slower than the overall tumbling have been explored more recently, in particular by exploiting residual dipolar couplings (RDCs)[21−23] in combination with computational approaches.[24,25] A normal mode has been identified as the main source of conformational diversity in ubiquitin,

whether it is free or bound in complexes, suggesting a conformational selection mechanism for binding.[24]

Recent studies of the structural diversity of ubiquitin[26] and its mutants[27] have convincingly identified the main mechanism of conformational exchange: a flip of the backbone of residues Asp52-Gly53 coupled with the formation of a H-bond between the side-chain carboxyl group of Glu24 and the backbone H^N of Gly53. Yet, some dynamic features still resist a mechanistic interpretation. The effect of chemical exchange on the relaxation of multiple quantum coherences (MQCs) has been shown to provide an exquisitely sensitive probe of motions.[13,14,18,19] Here, we use our heteronuclear double resonance (HDR) method[28−30] to determine the time scales of microsecond motions in ubiquitin using a large number of probes. We show that most motions occur on the same time scale. We suggest that a small tilt of the α-helix, which may be modulated by the dynamics of H-bonds at both ends, may explain our observations.

Correlated chemical exchange experienced by two nuclear spins has a distinct effect on the relaxation of zero- and double-quantum coherences.[31] Cross-correlation of chemical shift modulations (CSM) can be identified as long as appropriate MQCs can be excited and converted to observable coherence, in pairs of nuclei separated by one bond[32−34] or up to three bonds.[14,35,36] Correlated processes on millisecond time scales have been characterized in various proteins using relaxation dispersion techniques employing trains of spin echoes with variable pulse repetition rates.[18,19,37] Recently, we have shown that HDR methods allowed the quantification of time scales in the microsecond range in backbone NH^N pairs.[28] Interestingly, the signature of correlated chemical exchange is significantly more pronounced than in single-quantum studies of ubiquitin.[13] This is illustrated in Figure 1a, where the contributions of chemical exchange to the transverse relaxation of backbone ^{15}N nuclei (R_{ex}) are derived from the comparison of transverse autorelaxation rates (R_2) and cross-correlated cross-relaxation rates (η_{xy}).[38] Several auto- and cross-correlated relaxation mechanisms contribute to the cross-relaxation rate μ_{MQ} that describes the interconversion of operators $2N_xH_x$ and $2N_yH_y$.[31] Values of μ_{MQ} that differ significantly from the average for a given protein and isotope labeling scheme are typically
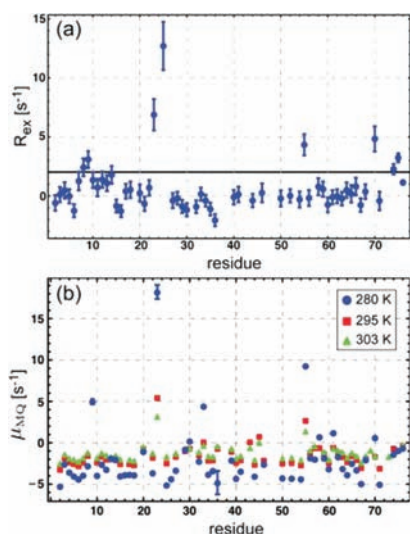
Figure 1. Identification of chemical exchange contributions to the relaxation of single- and multiple-quantum coherences in ubiquitin. (a) Contributions R_{ex} of chemical exchange to the nitrogen-15 transverse relaxation rates at 280 K. The rates R_2 were measured using a Carr−Purcell−Meiboom−Gill (CPMG) echo train, and rates η_{xy} were determined using a symmetrical reconversion method.[39] The expression $R_{ex} = R_2 - \kappa\eta_{xy}$ was used with $\kappa = 1.31$. The value of κ was derived from the correlation of R_2 and η_{xy} excluding the residues with the 15 lowest and the 15 highest values of R_2. (b) Cross-relaxation rates μ_{MQ} measured with the pulse sequence of Kloiber and Konrat[32] (K&K) at 280 K (blue circles), 295 K (red squares), and 303 K (green triangles).

Figure 2. Dispersion profiles for nine NH^N pairs in ubiquitin at 280 K. (a) Profiles for the NH^N pairs of Thr9, Ile23, and Thr55; (b) profiles for the NH^N pairs of Ile30, Lys33, and Asp58; (c) profiles for the NH^N pairs of Ile61, Val70 and the overlapped signals of Leu43 and Phe45. The point at $\omega_1/(2\pi) = 0$ Hz was obtained with K&K experiments; all other data were obtained with HDR with two on-resonance rf fields. The solid lines correspond to a global fit to eq 1 with the genetic algorithm (GA) discussed in the text and SI. Each dispersion profile required 36 h to 6 days of experimental time.

interpreted by invoking a correlated chemical exchange process.[13,32] As can be seen in Figure 1b, evidence of exchange can be found for many NH^N pairs.

We have explored the time scale of chemical exchange processes in all NH^N pairs with a cross-relaxation rate $\mu_{MQ} \geq 0$ s^{-1} at 280 K. Figure 2 shows dispersion profiles measured in a sample of perdeuterated and uniformly ^{15}N labeled human ubiquitin (1.5 mM, pH 6.8) at 280 K on an 800 MHz Bruker Avance spectrometer equipped with a TXI cryoprobe with z-axis gradients. The HDR pulse sequence is described in the Supporting Information (SI). For each selected NH^N pair, a full dispersion profile was recorded by placing the carrier frequencies on-resonance for both proton and nitrogen-15 channels. A temperature compensation scheme was used so that heating by rf pulses was constant for all mixing times. Potential variations in temperature were monitored by recording series of heteronuclear single quantum coherence (HSQC) spectra[40] at 280−297 K. Differences in chemical shifts of some selected pairs of resonances were fitted to a linear function of temperature. These differences were then monitored throughout the measurement of a full dispersion profile. The lowest temperature was found in K&K experiments (279.4 ± 0.7 K) while the highest (280.0 ± 0.7 K) was measured in HDR experiments with the highest rf amplitude and the longest relaxation delay: $\omega_1/(2\pi) = 2.9$ kHz and $T_{rel} = 50$ ms. Such small variations do not preclude a quantitative analysis (see SI).

Figure 2 shows all measured dispersion profiles. The μ_{MQ} rates measured with the K&K sequence of Kloiber and Konrat[32] (Figure 1b) were assumed to correspond to negligible effective rf fields, with $\mu_{MQ}^{eff} = \mu_{MQ}/2$, where the factor 1/2 takes into account the averaging effect of the rf fields on the
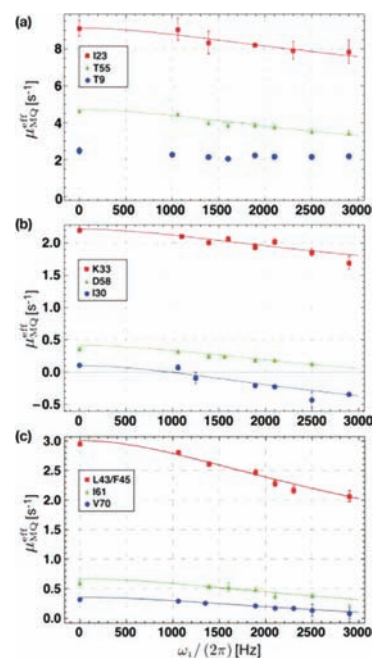
relaxation superoperator.[30] This approach is valid in the absence of slower chemical exchange processes contributing to μ_{MQ}. With the exception of Thr9, all profiles show a small decrease of μ_{MQ} with increasing rf amplitude, indicating the presence of exchange processes with rates comparable to the maximum rf amplitudes employed: $k_{ex} \geq 18\,000$ s^{-1}; with $k_{ex} = k_{AB} + k_{BA}$ for a two-site exchange between sites A and B. Dispersion profiles were fitted to the expression derived for fast two-site exchange under HDR-WALTZ-32 irradiation:[28]

$$\mu_{MQ}^{eff}(\omega_1) = \mu_{MQ}^0 + \frac{\overline{\Delta\Omega} \cdot \tau_{ex}}{1 + \omega_1^2\tau_{ex}^2}\left[1 + \frac{23\omega_1^3\tau_{ex}^3}{16\pi\left(1 - \exp(-8\tau_R/\tau_{ex})\left(1 + \omega_1^2\tau_{ex}^2\right)\right)}\right] \quad (1)$$

where μ_{MQ}^0 is the value of μ_{MQ}^{eff} in the absence of exchange; $\tau_{ex} = 1/k_{ex}$; ω_1 is the amplitude of the matched rf fields applied to both channels; $\tau_R = 12\pi/\omega_1$ is the duration of a single WALTZ-32 composite pulse; and $\overline{\Delta\Omega} = p_A p_B \Delta\Omega_{AB}^H \Delta\Omega_{AB}^N$; with the populations p_A and p_B of sites A and B ($p_A + p_B = 1$); $\Delta\Omega_{AB}^N$ (or $\Delta\Omega_{AB}^H$) the difference of resonance frequency for the nitrogen-15 nuclei (or protons) between sites A and B. A genetic algorithm (GA) implemented in Mathematica[41] and is described in detail in SI.

The data presented in Figure 1 offer complementary information about a complex pattern of chemical exchange processes in ubiquitin. Single-quantum relaxation rates (Figure 1a) show the presence of chemical exchange in the hydrophobic patch (Leu8, Thr9, Val70) at the N-terminus of helix $\alpha 1$ (Ile23 and Asn25; the signal of Glu24 being too weak) and in the $\beta 4$-$\alpha 2$ loop (Thr55).[42] Multiple-quantum rates (Figure 1b) confirm exchange for Thr9, Ile23, Thr55, and Val70 and provide further evidence of chemical exchange at the C-

terminus of helix $\alpha1$ (Ile30 and Lys33) as well as in helix $\alpha2$ (Asp58) and in loop $\alpha2$-$\beta5$ (Ile61). Residues with small contributions of chemical exchange can be identified from the temperature dependence of μ_{MQ}. Indeed, as the temperature decreases, the viscosity of water increases, which leads to an increase in the magnitude of μ^0, in agreement with the general trend. Contributions of fast chemical exchange to relaxation also increase with decreasing temperature. Depending on the relative signs of the chemical shift changes $\Delta\Omega_{AB}^N$ and $\Delta\Omega_{AB}^H$, these two effects will lead to a particular temperature dependence of μ_{MQ} (either enhanced or reduced). In light of these effects, small contributions of chemical exchange can also be identified for residues Ile13, Thr14, Ser20, Lys29, Ala46, Ile56, Tyr59, Gln62, and His68. Finally, the NH^N pairs of Leu43 and Phe45 show signatures of chemical exchange at 295 K, but their signals overlap at 280 K.

Chemical exchange that is not evident from our single quantum rates (Figure.1a) can be detected by the K&K method (Figure 1b). This may be interpreted in two ways: *either* the time scale of the exchange process is much slower than 1 ms (the pulse repetition interval of the CPMG sequence) *or* large *proton* chemical shift modulations make multiple-quantum experiments more sensitive. The determination of time scales with HDR (Figure 2) as well as an earlier analysis[16] of microsecond motions in ubiquitin at 278 K show that the latter interpretation must be correct.

The results of the global fit of the dispersion profiles shown in Figure 2 are presented as SI. With the exception of the flat profile obtained for Thr9, all dispersion curves can be fitted to eq 1. The fitted rate for the exchange process $k_{ex} = (19 \pm 1) \times 10^3$ s^{-1} can be compared with the time scales of individual fits (see SI), with an average 18 800 s^{-1} and a standard deviation of 900 s^{-1}. Based on the corrected Aikake Information Criterion (AICc), the global model has a probability of >99% of reproducing the data better than the individual fits. This time scale is in good agreement with single-quantum rates[13,20] (see SI). Identical time scales are not sufficient to prove correlated motions, as has been shown in studies of RNase A.[45,46] Yet evidence of a common time scale invites us to speculate about possible mechanisms of correlated dynamics. Figure 3
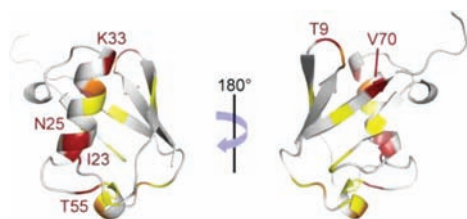

Figure 3. Chemical exchange contributions to relaxation rates mapped onto the structure of ubiquitin. Residues rendered in red show large contributions to SQ ($R_{ex} > 4$ s^{-1}) or MQ ($\mu_{MQ} > 4$ s^{-1}) relaxation rates; those represented in orange show contributions above the threshold in either SQ ($R_{ex} > 2.25$ s^{-1}) or MQ measurements ($\mu_{MQ} > 0$ s^{-1}), while residues in yellow feature a nontrivial temperature dependence of μ_{MQ}. A solution-state structure of ubiquitin[43] (pdb code 1d3z), and PYMOL[44] were employed to generate images.

represents residues in ubiquitin for which contributions of chemical exchange to SQ or MQ relaxation rates have been identified. The largest effects are seen at both ends of helix $\alpha1$ as well as at the two main interaction sites:[47] the hydrophobic patch and the loops and helix between $\beta4$ and $\beta5$. The motions

of the N-terminus of helix $\alpha1$ and the $\beta4$-$\alpha2$ loop are coupled through H-bonds between the side chain carboxyl of Glu24 and the backbone H^N of Gly53[26,27] as well as between the backbone H^N of Ile23 and the backbone CO of Arg54.[13] This motion is likely to be coupled with the dynamics of Thr55 and Asp58 by a H-bond between the side chain carboxyl group of Asp58 and the backbone H^N of Thr55 (see Figure 4b). At the C-terminal end of helix $\alpha1$, the H-bond between the H^N of Lys33 and the CO of Lys29 couples the motions of the peptide planes comprising the Lys33 and Ile30 NH^N pairs.
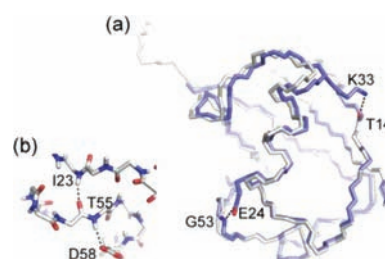

Figure 4. Relevant H-bonds for the propagation of motions in ubiquitin. (a) The solution state (gray, pdb code 1d3z) and crystal structures (blue, pdb code 3ons) of ubiquitin were aligned to minimize deviations of the β sheets. The H-bonds at both ends of the helix $\alpha1$ are shown. (b) Network of H-bonds that is likely to contribute to the propagation of motions between the N-terminus of helix $\alpha1$, loop $\beta4$-$\alpha2$, and helix $\alpha2$.

The possible coupling of the motions of the N- and C-termini of helix $\alpha1$ should also be considered. For instance, the G53A mutation leads to a significant enhancement of the contribution of chemical exchange to the transverse SQ relaxation of the backbone nitrogen-15 nuclei of Ala28 and Lys33.[27] In addition, although intermolecular contacts may also be considered, the presence of a highly populated Glu24-Gly53 H-bond in the microcrystalline form of ubiquitin[26] is correlated with significant changes in the chemical shift of the backbone ^{15}N of Lys33.[48] Comparison of the solution state structure[43] (pdb code 1d3z) and solid state structure[26] (pdb code 3ons) also reveals the presence of an additional H-bond between the side-chain ammonium group of Lys33 and the backbone CO of Thr14. The existence of this H-bond has been confirmed by MD simulations[49] and experiments in solution.[50] Alignment of the β-sheets of the two structures (Figure 4a) offers interesting insight into the conformational transition. The helix $\alpha1$ is slightly tilted, as if it were pulled on one side by the Glu24-Gly53 H-bond and on the other side by the Lys33-Thr14 H-bond. The distances between the C$^\alpha$ in the two structures are 0.5 Å for Glu24 and 1.1 Å for Lys33. The dynamic nature of helix $\alpha1$ has been observed in several studies.[51-53] Note that the tilt between the two structures is small, on the order of 5°, which would be less than previously reported,[51] and could possibly be a projection of a more complex motion.[24]

Further correlations of motions, in particular between the β-sheet and helix $\alpha1$, remain hypothetical. However, in contradiction to what would be expected if motions at distinct bonding sites were coupled,[54,55] a study of a ternary complex of ubiquitin failed to detect any allosteric effect between the hydrophobic patch and the $\beta4$-$\alpha2$ loop interfaces.[56] Surprisingly, the picture of motions in ubiquitin derived from our chemical-exchange based study seems different from the one drawn from the analysis of RDCs.[25] This underlines the diversity of motions in ubiquitin as RDCs are more sensitive to

fluctuations of the major conformer, while our work focuses on transitions to a weakly populated excited state.

ASSOCIATED CONTENT

S Supporting Information

Details of the HDR pulse sequence; temperature calibration; individual fits of dispersion curves; effect of temperature changes, single-quantum dispersion, genetic algorithm used to fit dispersion curves. This material is available free of charge via the Internet at http://pubs.acs.org.

AUTHOR INFORMATION

Corresponding Author
Fabien.Ferrage@ens.fr

Present Address
[⊥]Bruker BioSpin AG, Industriestrasse 26, 8117 Fällanden, Switzerland.

ACKNOWLEDGMENTS

REFERENCES

(1) Henzler-Wildman, K.; Kern, D. *Nature* **2007**, *450*, 964.
(2) Eisenmesser, E. Z.; Millet, O.; Labeikovsky, W.; Korzhnev, D. M.; Wolf-Watz, M.; Bosco, D. A.; Skalisky, J. J.; Kay, L. E.; Kern, D. *Nature* **2005**, *438*, 117.
(3) Watt, E. D.; Shimada, H.; Kovrigin, E. L.; Loria, J. P. *Proc. Natl. Acad. Sci. U.S.A.* **2007**, *104*, 11981.
(4) Bhabha, G.; Lee, J.; Ekiert, D. C.; Gam, J.; Wilson, I. A.; Dyson, H. J.; Benkovic, S. J.; Wright, P. E. *Science* **2011**, *332*, 234.
(5) Boehr, D. D.; McElheny, D.; Dyson, H. J.; Wright, P. E. *Science* **2006**, *313*, 1638.
(6) Boehr, D. D.; Nussinov, R.; Wright, P. E. *Nat. Chem. Biol.* **2009**, *5*, 789.
(7) Mittermaier, A.; Kay, L. E. *Science* **2006**, *312*, 224.
(8) Palmer, A. G. *Chem. Rev.* **2004**, *104*, 3623.
(9) Schneider, D. M.; Dellwo, M. J.; Wand, A. J. *Biochemistry* **1992**, *31*, 3645.
(10) Tjandra, N.; Feller, S. E.; Pastor, R. W.; Bax, A. *J. Am. Chem. Soc.* **1995**, *117*, 12562.
(11) Showalter, S. A.; Bruschweiler, R. *J. Chem. Theory Comput.* **2007**, *3*, 961.
(12) Maragakis, P.; Lindorff-Larsen, K.; Eastwood, M. P.; Dror, R. O.; Klepeis, J. L.; Arkin, I. T.; Jensen, M. O.; Xu, H. F.; Trbovic, N.; Friesner, R. A.; Palmer, A. G.; Shaw, D. E. *J. Phys. Chem. B* **2008**, *112*, 6155.
(13) Massi, F.; Grey, M. J.; Palmer, A. G. III. *Protein Sci.* **2005**, *14*, 735.
(14) Majumdar, A.; Ghose, R. *J. Biomol. NMR* **2004**, *28*, 213.
(15) Pelupessy, P.; Ferrage, F.; Bodenhausen, G. *J. Chem. Phys.* **2007**, *126*, 134508.
(16) Hansen, D. F.; Feng, H. Q.; Zhou, Z.; Bai, Y. W.; Kay, L. E. *J. Am. Chem. Soc.* **2009**, *131*, 16257.
(17) Mills, J. L.; Szyperski, T. *J. Biomol. NMR* **2002**, *23*, 63.
(18) Dittmer, J.; Bodenhausen, G. *J. Am. Chem. Soc.* **2004**, *126*, 1314.
(19) Wist, J.; Frueh, D.; Tolman, J. L.; Bodenhausen, G. *J. Biomol. NMR* **2004**, *28*, 263.
(20) Ban, D.; et al. *Angew. Chem., Int. Ed.* **2011**, *50*, 11437.
(21) Peti, W.; Meiler, J.; Brüschweiler, R.; Griesinger, C. *J. Am. Chem. Soc.* **2002**, *124*, 5822.
(22) Lakomek, N. A.; Walter, K. F. A.; Fares, C.; Lange, O. F.; de Groot, B. L.; Grubmuller, H.; Bruschweiler, R.; Munk, A.; Becker, S.; Meiler, J.; Griesinger, C. *J. Biomol. NMR* **2008**, *41*, 139.
(23) Salmon, L.; Bouvignies, G.; Markwick, P.; Blackledge, M. *Biochemistry* **2011**, *50*, 2753.
(24) Lange, O. F.; Lakomek, N. A.; Fares, C.; Schroder, G. F.; Walter, K. F. A.; Becker, S.; Meiler, J.; Grubmuller, H.; Griesinger, C.; de Groot, B. L. *Science* **2008**, *320*, 1471.
(25) Fenwick, R. B.; Esteban-Martin, S.; Richter, B.; Lee, D.; Walter, K. F. A.; Milovanovic, D.; Becker, S.; Lakomek, N. A.; Griesinger, C.; Salvatella, X. *J. Am. Chem. Soc.* **2011**, *133*, 10336.
(26) Huang, K. Y.; Amodeo, G. A.; Tong, L. A.; McDermott, A. *Protein Sci.* **2011**, *20*, 630.
(27) Sidhu, A.; Surolia, A.; Robertson, A. D.; Sundd, M. *J. Mol. Biol.* **2011**, *411*, 1037.
(28) Ulzega, S.; Salvi, N.; Segawa, T. F.; Ferrage, F.; Bodenhausen, G. *ChemPhysChem* **2011**, *12*, 333.
(29) Verde, M.; Ulzega, S.; Ferrage, F.; Bodenhausen, G. *J. Chem. Phys.* **2009**, *130*, 074505.
(30) Ulzega, S.; Verde, M.; Ferrage, F.; Bodenhausen, G. *J. Chem. Phys.* **2009**, *131*, 224503.
(31) Frueh, D. *Prog. NMR Spectrosc.* **2002**, *41*, 305.
(32) Kloiber, K.; Konrat, R. *J. Biomol. NMR* **2000**, *18*, 3342.
(33) Frueh, D.; Tolman, J. R.; Bodenhausen, G.; Zwahlen, C. *J. Am. Chem. Soc.* **2001**, *123*, 4810.
(34) Del Rio, A.; Anand, A.; Ghose, R. *J. Magn. Reson.* **2006**, *180*, 1.
(35) Pelupessy, P.; Ravindranathan, S.; Bodenhausen, G. *J. Biomol. NMR* **2003**, *25*, 265.
(36) Lundstrom, P.; Mulder, F. A. A.; Akke, M. *Proc. Natl. Acad. Sci. U.S.A.* **2005**, *102*, 16984.
(37) Orekhov, V. Y.; Korzhnev, D. M.; Kay, L. E. *J. Am. Chem. Soc.* **2004**, *126*, 1886.
(38) Wang, C. Y.; Palmer, A. G. *Magn. Reson. Chem.* **2003**, *41*, 866.
(39) Pelupessy, P.; Espallargas, G. M.; Bodenhausen, G. *J. Magn. Reson.* **2003**, *161*, 258.
(40) Bodenhausen, G.; Ruben, D. J. *Chem. Phys. Lett.* **1980**, *69*, 185.
(41) Wolfram Research, I., version 8.0 ed.; Champaign, IL, 2010.
(42) Chemical exchange also seems to be detected for the very mobile residues Leu73 and Arg74; these contributions are possibly due to proton exchange.
(43) Cornilescu, G.; Marquardt, J. L.; Ottiger, M.; Bax, A. *J. Am. Chem. Soc.* **1998**, *120*, 6836.
(44) Schrodinger, L. PYMOL, version 0.99rc6 ed.; Schrödinger, LLC.
(45) Cole, R.; Loria, J. P. *Biochemistry* **2002**, *41*, 6072.
(46) Doucet, N.; Khirich, G.; Kovrigin, E. L.; Loria, J. P. *Biochemistry* **2011**, *50*, 1723.
(47) Dikic, I.; Wakatsuki, S.; Walters, K. J. *Nat. Rev. Mol. Cell Biol.* **2009**, *10*, 659.
(48) Igumenova, T. I.; Wand, A. J.; McDermott, A. E. *J. Am. Chem. Soc.* **2004**, *126*, 5323.
(49) Esadze, A.; Li, D. W.; Wang, T. Z.; Bruschweiler, R.; Iwahara, J. *J. Am. Chem. Soc.* **2011**, *133*, 909.
(50) Zandarashvili, L.; Li, D. W.; Wang, T. Z.; Bruschweiler, R.; Iwahara, J. *J. Am. Chem. Soc.* **2011**, *133*, 9192.
(51) Meiler, J.; Peti, W.; Griesinger, C. *J. Am. Chem. Soc.* **2003**, *125*, 8072.
(52) Kitahara, R.; Yokoyama, S.; Akasaka, K. *J. Mol. Biol.* **2005**, *347*, 277.
(53) Vogeli, B.; Segawa, T. F.; Leitz, D.; Sobol, A.; Choutko, A.; Trzesniak, D.; van Gunsteren, W.; Riek, R. *J. Am. Chem. Soc.* **2009**, *131*, 17215.
(54) Gunasekaran, K.; Ma, B.; Nussinov, R. *Proteins: Struct., Funct., Bioinf.* **2004**, *57*, 433.
(55) Long, D.; Brüschweiler, R. *J. Am. Chem. Soc.* **2011**, *133*, 18999.
(56) Garner, T. P.; Strachan, J.; Shedden, E. C.; Long, J. E.; Cavey, J. R.; Shaw, B.; Layfield, R.; Searle, M. S. *Biochemistry* **2011**, *50*, 9076.